ON THE INTERPRETATION OF MEASURED PROFILE LOSSES IN UNSTEADY WAKE-TURBINE BLADE INTERACTION STUDIES

HP Hodson and WN Dawes
Whittle Laboratory
Cambridge University Engineering Department
Madingley Road
Cambridge CB3 ODY
England

ABSTRACT

The interaction of wakes shed by a moving bladerow with a downstream bladerow causes unsteady flow. The meaning of the freestream stagnation pressure and stagnation enthalpy in these circumstances has been examined using simple analyses, measurements and CFD. The unsteady flow in question arises from the behaviour of the wakes as so-called negative-jets. The interactions of the negative-jets with the downstream blades lead to fluctuations in static pressure which in turn generate fluctuations in the stagnation pressure and stagnation enthalpy. It is shown that the fluctuations of the stagnation quantities created by unsteady effects within the bladerow are far greater than those within the incoming wake. The time-mean exit profiles of the stagnation pressure and stagnation enthalpy are affected by these large fluctuations. This phenomenon of energy separation is much more significant than the distortion of the time-mean exit profiles that is caused directly by the cross-passage transport associated with the negative-jet, as described by Kerrebrock and Mikolajczak. Finally, it is shown that if only time-averaged values of loss are required across a bladerow, it is nevertheless sufficient to determine the time-mean exit stagnation pressure.

NOMENCLATURE

h enthalpy
$\dot{m}$ mass flow rate
P pressure
$\dot{Q}$ rate of heat transfer inwards
ρ density
R gas constant
s entropy
τ periodic time
T thermodynamic temperature
t time
u velocity
ω vorticity
$\dot{W}_x$ power output

Subscripts and Superscripts

0 stagnation
1 inlet
2 exit
Δ change with respect to inlet conditions
$\bar{}$ mean value

INTRODUCTION

This paper considers the effects of unsteady inflow on the stagnation quantities at exit from a turbomachine bladerow. The unsteady flow in question arises because of the interactions of the flow fields associated with the stator and rotor bladerows.

One of the first studies of the effects of rotor-stator interactions upon the aerodynamic efficiency of a turbomachine was conducted by Lopatitskii et al (1969) using a single-stage axial flow turbine. They reported that, depending upon the blade geometry and Reynolds number, the rotor profile loss was between 2 and 4 times that of the same cascade operating with steady inflow. It is as a result of investigations such as these that the subject of rotor-stator interactions has received much attention during the past decade or so. The effect of upstream wakes on bladerow performance has been of particular interest at the Whittle Laboratory. This is known to be an important contributor to the differences noted between the performance of a given profile in cascade and turbomachine environments (Hodson (1989)).

The effect of unsteady flow on the loss (entropy creation) of a bladerow is not the main subject of this paper. However, the loss is usually determined from measurements of the stagnation pressure and stagnation temperature. Unfortunately, the unsteadiness arising from rotor-stator interactions also modifies the stagnation pressure and stagnation temperature fields, irrespective of any change in bladerow

efficiency. This problem and its consequences in the context of rotor-stator wake interactions are considered here.

One of the first studies of the interaction of rotor wakes with a stationary blade was conducted by Meyer (1958). Fig. 1 is a schematic interpretation of his model of the interaction in the context of a turbine rotor. Each wake is initially represented as a perturbation (the so-called "negative-jet") of a uniform flow. The wakes are transported with the main flow and are chopped into segments by the downstream bladerow. Within the passage, the wake segments continue to behave as negative-jets. The velocity induced by the negative-jet causes a build up of wake fluid on the suction and a removal of fluid from the pressure surface.

Kerrebrock and Mikolajczak (1970) observed that the circumferentially non-uniform stagnation temperature profile at the exit of a high Mach number compressor stator could be explained by assuming that the stagnation temperature is a convected scalar in unsteady flow. This is interpreted in the present context in fig. 1. Since the wake represents a defect in rotor-relative stagnation temperature, an increase in the same quantity is to be expected on the suction side of the passage with a commensurate decrease on the pressure side. Actual evidence of the kinematic behaviour of wakes in compressors can be found in the experimental data of Adachi and Murakami (1979) and Weyer and Dunker (1983) who, in independent studies, measured the velocity field within the passages of compressor stators.

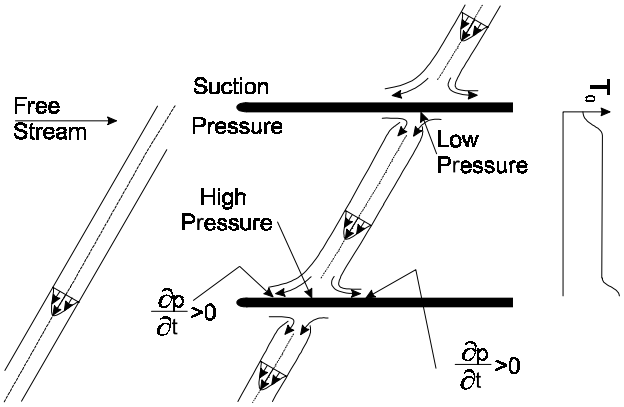

Fig. 1 The Representation of a Wake as a Negative Jet and Resulting Distortion of the Relative Stagnation Temperature Profile at exit from a Turbine Rotor

Smith (1966) noted that as a result of the blade circulation, the wake segments are sheared and stretched as they progress through the blade passage. These phenomena are particularly evident in axial turbines. In one of the first studies of wake-transport in axial turbines, Hodson (1985) traversed the flow within the rotor passage of an axial-flow turbine using hot-wire anemometers. To obtain a picture of the unsteady flow, the time-mean velocity data was subtracted from the phase-locked ensemble averages at each measurement location within the rotor passage. These experimental results and the subsequent numerical predictions of Hodson (1985), Giles (1987), Rai (1987), Korakianitis (1991) and Dawes (1993) confirm that simple kinematic theory can be used to explain the movement of wakes through downstream bladerows, whether in turbines or compressors.

Curtis et al (1996) have reported an experimental study of profile losses in low pressure turbine cascades that were subjected to incoming wakes. Fig. 2 shows an example of the data that were acquired ¼ axial chords downstream of a representative cascade using a conventional pressure probe. The results are typical of a large number of measurements. Apart from the blade wakes, the measured exit flow is characterised by non-uniform stagnation pressures in the "free-stream". An apparent loss of stagnation pressure appears as a lump towards the pressure side of the passage. An apparent gain (on the face of it violating the second law of thermodynamics) appears on the suction side. The incoming wakes represented a defect in cascade-relative stagnation pressure. Cross-passage transport in the negative-jet would be expected to create free-stream non-uniformities of the opposite sign. Therefore, the free-stream non-uniformities in fig. 2 cannot be explained using the Kerrebrock and Mikolajczak model (1970). Nor is it caused by unsteady effects on the probe used for the measurements. He (1994) presented a preliminary discussion of this problem. The primary purpose of this paper is to describe in detail the true mechanism.

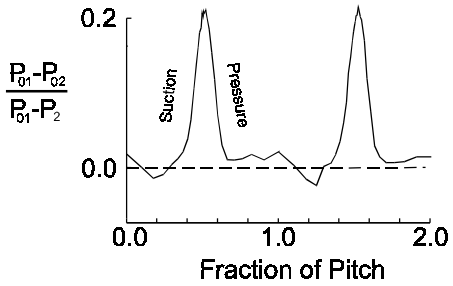

Fig. 2 Time-mean absolute stagnation pressure at ¼ axial chord downstream of blades - measured (see Curtis et al, 1996)

Much of the work on blade-wake interactions at the Whittle Laboratory has been carried out using large scale facilities. Since Reynolds numbers must be representative in such experiments, the use of large scale facilities usually means that the experiments are conducted at Mach 0.1 or less. At typical ambient stagnation conditions and at Mach 0.1, the static temperature is only 0.6 K lower than the stagnation temperature and the static pressure is about 700 Pa lower than the stagnation pressure. Systems capable of measuring pressure differences of this order, and much less, are readily available whereas equivalent temperature measurement systems are not. In practice, therefore, only stagnation pressure measurements are available with which to evaluate the entropy creation. Since it will be shown that unsteadiness affects the stagnation pressure and stagnation temperature fields, a secondary purpose of this paper is to discover whether the measurement of stagnation pressure alone is sufficient for the evaluation of thermodynamic loss.

METHODOLOGY

Numerical Simulation Using CFD

The numerical simulations that form the basis of this paper were performed with the unsteady Navier-Stokes solver presented by Dawes

(1993). This code solves the three-dimensional Reynolds-averaged Navier-Stokes equations on an unstructured, solution-adaptive mesh. The equations of motion are discretised to second order space accuracy on a cloud of tetrahedrons and integrated forwards in time using a standard four-step Runge-Kutta algorithm. A standard blend of second and fourth order artificial smoothing is applied, by way of a pressure switch.

The turbulence is represented by a low-Reynolds number form of the k-ε model. It is not known what capabilities this turbulence model might possess in the prediction of wake-blade interactions. In the context of steady flow, studies of wake development behind lobed mixers showed good agreement with accepted wake decay rates (Waitz et al, 1995). Nevertheless, the present study is very much about following the kinematics of the wake away from the blade boundary layers, rather than the details of the wake-boundary layer interaction itself, and so the approach is believed to be adequate. Applications of the calculation method to cylinder vortex shedding and to the wake-rotor interaction case of Hodson (1985) were reported in Dawes (1993), to an axial compressor stage interaction in Dawes (1994) and to a centrifugal compressor stage interaction in Dawes (1994b).

In the present study, for reasons of economy and simplicity, a thin spanwise slice of a two-dimensional cascade was simulated and a 1:1 ratio was assumed between upstream wakes and blade count. Table 1 gives further details of the calculated flow.

Experimental Details: Low-Speed Moving-Bar Cascade

The cascade wind tunnel is normally used to study the effects of wakes on the performance of turbine cascades. The wakes are shed from a moving bar system ahead of the blades. The facility is described by Curtis et al, (1996). The very low Mach numbers (typically <0.05) encountered in this facility means that it is impossible to make useful measurements of the change in stagnation temperature across the cascade. Therefore, only stagnation pressure measurements are available with which to evaluate the entropy creation. It is to explain the measurements of stagnation pressure in this facility that the present investigation was undertaken.

A Pitot probe placed downstream of the moving bars was intended to provide the reference cascade inlet stagnation pressure. However, by traversing the Pitot in the axial direction in the absence of the cascade, it was found that the effects of unsteadiness on the readings from this Pitot probe were significant at the selected measurement location for some of the data presented here. For this reason, the stagnation pressure loss and therefore the drag of the stationary bars was determined and this was then used to calculate the change in stagnation pressure across the moving bars. A comparison of the results of the calculation with experimental data (see Schulte and Hodson (1996)) shows that the calculation yields faithful values for the mixed-out stagnation pressure downstream of the moving bars.

Normally, a conventional pneumatic probe system (e.g., a Neptune tube connected by about a metre of small bore tubing to a Scanivalve system) is used to perform pitch-wise traverses at mid-span to measure the profile loss of the cascade. Here, a Kulite XCS062 (1.5 mm dia.) fast response pressure transducer was fitted to the inlet of a Pitot tube and was used to traverse the exit flow alongside the conventional pneumatic probe. The relatively low bar-passing frequency ensures a faithful measurement by the Kulite probe of the instantaneous fluctuations in stagnation pressure. The unsteady data is added to the data provided by the conventional probe to produce the 'instantaneous' exit stagnation pressure profiles. Only ensemble-average and time-mean data are reported in this paper. The traverses were performed at a distance 0.5 axial chords downstream of the trailing edge plane of the cascade.

The cascade contains airfoils that are typical of modern thin low pressure turbine blades operating at a typical cruise Reynolds number and flow coefficient. Whereas the cascade geometry and the inlet velocity triangle of the cascade was identical to that used by Curtis et al (1996), the diameter and spacing of the moving bars were doubled so that the wake was greater in intensity and the relative pitch of the bars and cascade was approximately unity. Under these conditions, the cascade simulates a stator blade subjected to incoming rotor wakes rather than the opposite situation investigated by Curtis et al. Table 2 provides details of the wakes shed by the moving bars.

RESULTS AND DISCUSSION

Theory

The question of the relevance of stagnation pressure measurements to assess entropy creation in the unsteady environment of turbomachines has received little attention in the literature. Only the work of Epstein et al (1989) is known to the authors. They examined the effect of potential interactions between compressor rotor and stator blades on the measurement of rotor efficiency. Their study shows how the difference between the actual and the perceived adiabatic efficiency of the rotor varies as the positions of a stagnation pressure probe and a stagnation temperature probe vary in the circumferential direction when placed between the rotor and stator blades. The present paper complements the study of Epstein et al.

As the wake-segments convect through a blade passage, they create fluctuations in the velocity and static pressure. These are especially pronounced near to the surface. Greitzer (1984) points out that kinematic model of Kerrebrock and Mikolajczak (1970) does not consider the effects of fluctuating static pressures on the time-mean stagnation quantities. Yet, it is well known that the stagnation enthalpy of a particle changes as it traverses an inviscid flow where the static pressure fluctuates. This may be written

$$\frac{Dh_0}{Dt} = \frac{1}{\rho}\frac{\partial p}{\partial t} \qquad (1)$$

Dean (1959) showed that the above form of the 1st Law of Thermodynamics is consistent with the fact that in the case of a turbine rotor, where the stagnation enthalpy falls, a stationary observer would see, at a fixed viewpoint, a decreasing pressure with time (i.e., $\partial p / \partial t < 0$) as first the pressure side and then the suction side of the passage passes the observer's viewpoint.

The 2nd Law of Thermodynamics relates changes in stagnation pressure and stagnation enthalpy by

$$T_0 ds = dh_0 - \frac{1}{\rho_0} dp_0 \qquad (2)$$

where s is the entropy. Eqns. (1) and (2) together reveal that whenever the flow is unsteady, the stagnation enthalpy (or stagnation temperature) and the stagnation pressure of a given particle may not in general remain constant, even if the flow is isentropic. In particular,

changes in stagnation temperature may generate commensurate changes in stagnation pressure without affecting the thermodynamic loss. The phenomenon of energy separation, as this effect is sometimes called, is often found in von Karman vortex streets.

Unsteady flow field

For convenience, the computational domain is taken to represent the absolute frame of reference and the wake, the relative frame of reference in the discussion that follows.

Considerable insight into the flowfield was obtained from the numerical simulations. Fig. 3 shows a composite view of the unsteady velocity vectors (instantaneous minus the time-mean) and the entropy field at a certain instant in time. Plots such as these have been used by many authors to describe wake-blade interactions. The entropy contours are plotted as the quantity

$$P_{01}\exp\left(-\frac{s-s_1}{R}\right) \qquad (3)$$

where P_{01} and s_1 are the time-mean values at inlet. The above quantity represents the entropy within the flow as an equivalent (stagnation) pressure. Since entropy is convected by the flow, the incoming wakes may be identified by lower values of the above quantity. The entropy contours of fig. 3 show that as a wake shed from a moving source passes through the computational domain, it experiences the bowing, chopping, stretching and shearing which may be explained using kinematic principles. Owing to the relatively high loading of this bladerow, the distortion of the wake segments is very pronounced.

In the case of a compressor, Kerrebrock and Mikolajczak argued that variations in the time-mean stagnation temperature field at exit from a stator downstream of a rotor may be accounted for by examining the redistribution of flow that takes place due to the unsteady velocity field (see fig. 1). In the present study the maximum perturbation in absolute velocity at inlet amounts to 13.5 percent of the mean exit velocity (25.5 percent of the mean inlet velocity). The unsteady velocity vectors of fig. 3 reveal the existence of the so-called 'negative jet' at inlet to the bladerow. It also shows that this phenomenon persists as the wakes progress through the bladerow. As expected, a recirculating velocity field is established on each side of the wake as the wake enters the bladerow. The cross-passage transport tends to move fluid and therefore entropy from the pressure toward the suction side of the blade passage. This was shown schematically in fig. 1.

The maximum unsteady velocity in fig. 3 is 17 percent of the mean exit velocity (similar to that at the inlet) and is to be found near the centre-line of the wakes between the regions labelled A and C. This magnitude is a measure of the strength of the cross-passage transport. From fig. 3, it can be seen that approximately one wake passing cycle is required to convect the bulk of the wake-segment through the blade passage. In this time, a particle at the centre-line of the wake will have moved a maximum distance equivalent only to approximately 1/4 pitch relative to the adjacent free stream. The movement is towards the suction side of the passage. It causes an increase in the time-averaged entropy (loss) on the suction side of the passage, and a decrease on the pressure side as free-stream fluid replaces the wake fluid.

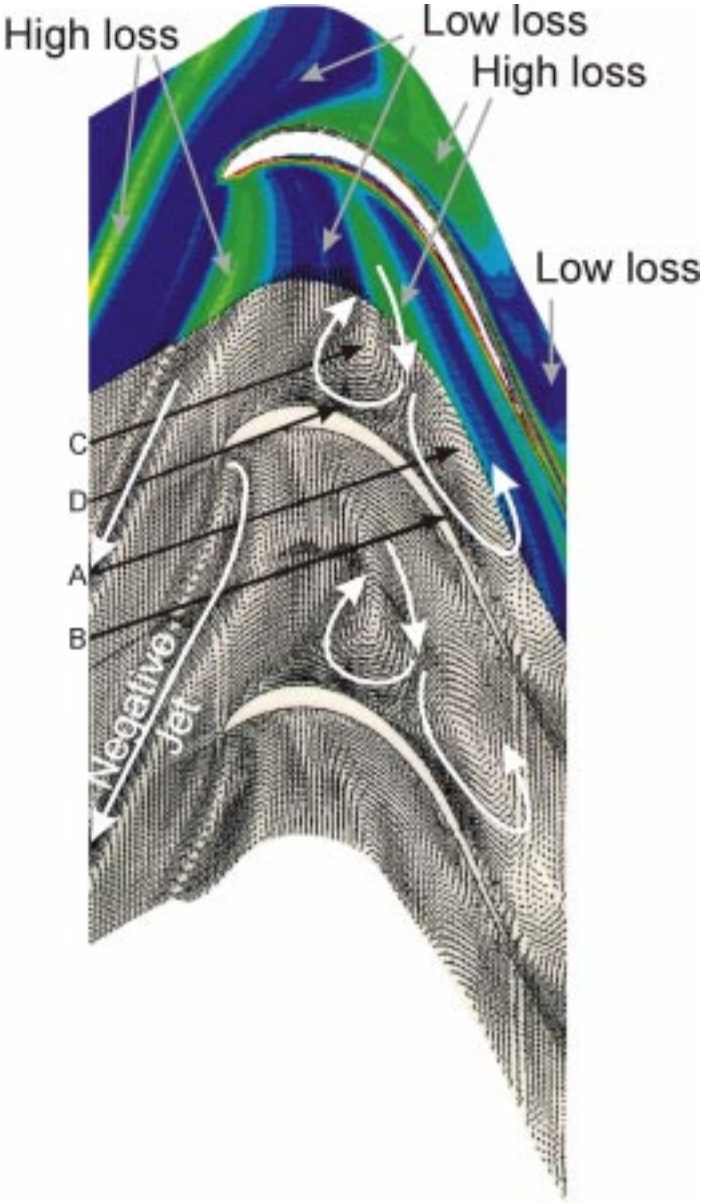

Fig. 3 Predicted contours of entropy and unsteady velocity vectors at one instant in time (contours increase cyclically through black, grey, white)

Fig. 4 presents the predicted pitchwise distribution of the entropy at ½ axial chord downstream of the cascade. The entropy is plotted as a loss coefficient based on the quantity defined in eqn. (3). The time-mean, maximum and minimum values are shown across two blade pitches. Fig. 4 shows that relative to the mean, wake fluid (i.e., loss) has on average accumulated toward the suction side of the passage (higher loss) while freestream fluid has accumulated toward the pressure side of the passage (lower loss). Between the wakes, the predicted mean value rises approximately from $-0.014(\bar{P}_{01}-P_2)$ to $0.024(\bar{P}_{01}-P_2)$. If the lower half (i.e. suction side) of each passage were to contain all of the incoming wake fluid, the mean value of loss (neglecting any entropy

creation) would be approximately $0.035(\bar{P}_{01}\text{-}P_2)$ in this half of the passage, with an equally negative value of $-0.035(\bar{P}_{01}\text{-}P_2)$ in the other half. The predicted freestream variation in time-mean entropy (loss) is consistent with the magnitude of the cross-passage transport velocities noted above.

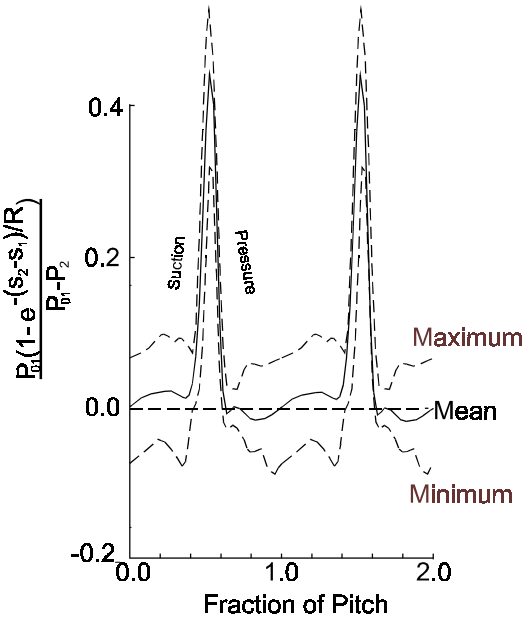

Fig. 4 Time-mean, maximum and minimum entropy at ½ axial chord downstream of blades - predicted

The effect of the cross-passage transport can also be seen in the amplitude of the entropy fluctuations as indicated by the difference between the maximum and minimum values. In the free-stream, near the pressure side of the wake, this difference has diminished. Elsewhere in the freestream, the amplitude is almost constant. The reduction near the pressure side suggests that the each wake has moved approximately 1/4 pitch relative to the adjacent free stream by the time it reaches the location corresponding to fig. 4.

Table 1 shows that in the wake-relative frame of reference, the wake appears as a reduction in stagnation pressure ($0.05\bar{P}_{01\text{rel}}$) with constant stagnation temperature. In the absolute frame of reference, the wake appears to the cascade as a region of low stagnation pressure ($\Delta P_{0\max} = 0.019 P_{01}$) and a region of low stagnation temperature ($\Delta T_{0\max} = 0.0059 T_{01}$), so that the fluctuations in stagnation pressure and stagnation temperature contribute equally to the fluctuations in entropy. If the cross-passage transport model of Kerrebrock and Mikolajczak were to be applied to the convection of the stagnation temperature (enthalpy) and stagnation pressure within the wakes, then in the absence of any other effects, freestream time-mean exit distributions similar to that of the entropy (see fig. 4) would be expected as the incoming wake has a deficit of these stagnation quantities.

Fig. 5 and fig. 6 present the predicted distributions of absolute stagnation temperature and absolute stagnation pressure at ½ axial chord downstream of the cascade. Time-mean, maximum and minimum variations and rms fluctuations are shown as coefficients. A comparison of the two figures shows that in general, the distributions of the time-mean values are very similar in the free-stream. The highest values are to be found nearer the pressure side while the lowest occur toward the suction side. These variations do not in general mimic the loss (entropy) variations in the free stream shown in fig. 4. Therefore, a mechanism must exist which not only causes an effect that is opposite in sign to that of the negative-jet but also is of greater significance. An examination of the unsteady entropy field, which is the approach favoured by many authors, cannot reveal this mechanism.

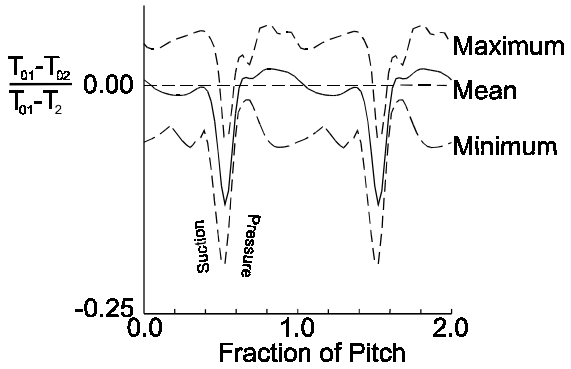

Fig. 5 Time-mean, maximum and minimum absolute stagnation temperature at ½ axial chord downstream of blades - predicted

Comparing the maximum amplitudes of the stagnation quantities in fig. 5 and fig. 6 with the inlet deficits given in Table 1 shows that the maximum amplitudes of the stagnation pressure and stagnation temperature fluctuations are predicted to be about twice those which arise in the inlet flow. Furthermore, the pitchwise variations of the amplitude of the stagnation pressure and stagnation temperature (enthalpy) within the freestream also show a degree of similarity. These observations suggest that the mechanism that is sought must lie in the unsteady physics associated with the stagnation enthalpy transport equation (eqn. (1)).

At this point, it is useful to compare the measured unsteady exit flow data with that predicted to demonstrate some confidence in the numerical simulations and any interpretations that arise from them. Time-mean, maximum, minimum and rms fluctuations of the measured exit ensemble-average stagnation pressures are shown in fig. 7. A comparison of the predictions in fig. 6 with the measurements of fig. 7 is encouraging. In the freestream, the pitchwise variation of the time-mean is well predicted and the rms fluctuations are in good quantitative agreement. The very large unsteady envelope is well represented. The rms distribution shown in fig. 6 and fig. 7 show that the fluctuations in stagnation pressure are greater almost everywhere at exit than at inlet to the cascade. Indeed, the maximum-minimum variation is rather larger than the depth of the cascade wakes.

Fig. 8 shows the time-histories of the measured ensemble-average stagnation pressures at inlet (top trace) and at various pitchwise locations across the exit traverse plane (lower traces). The exit locations are numbered 1 to 6 and are shown in fig. 7. Three wake-passing cycles are shown in each trace. It can be clearly seen that the fluctuations in the traces at exit are much larger than those at inlet. Within the free-stream (locations 2-5), the increased magnitude of the fluctuations must have their origin within the unsteady fluid dynamics of the flow field.

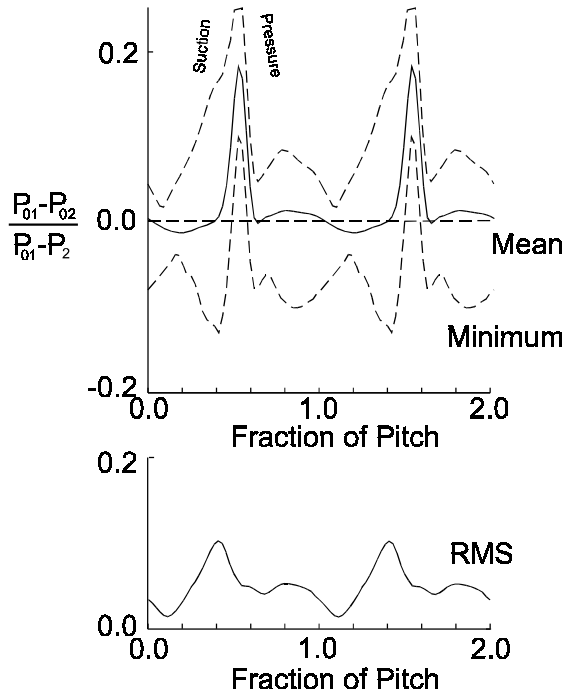

Fig. 6 Time-mean, maximum, minimum and rms absolute stagnation pressure ½ axial chord downstream of blades - predicted

The key to understanding the unsteady phenomenon lies in an exploration of the predicted unsteady (instantaneous minus time-mean) static pressure field and its variation with time. The time-mean static pressure field is of much less consequence. Contours of the unsteady static pressure for the same instant as in fig. 3 are plotted in the lower part of fig. 9. The pressure perturbations within the passage arise largely as a result of the recirculating unsteady velocity field that is established within the blade passage. The centre of rotation on the downstream side of the wake (region A) is associated with a region of low unsteady static pressure. At the instant shown, this region of low unsteady pressure extends across passage with the region of lowest unsteady pressure (region B) adjacent to the suction surface. A further, more localised and less pronounced region of low unsteady pressure is associated with the centre of the recirculating flow on the upstream side of the wake (region C) at this instant in time. Below region C is the region of highest unsteady static pressure. It is not a coincidence that this region (region D) is located near to where the centre-line of the negative jet impinges on the blade surface. The unsteady pressure decreases along the suction surface just upstream of region D.

An examination of the movement of regions A-D during a wake-passing cycle would reveal that these features arise as the wake enters the blade passage, or soon after, and that although their associated magnitudes change, they tend to convect with the main flow. Indeed, an examination of the unsteady blade-surface static pressures would show that the perturbations on the pressure side propagate at the same speed as the flow in the centre of the passage. On the suction side, a more complicated picture arises though again, a convective characteristic is discernible. Whilst recognising the pressure field to subject to more than just convective influences, the simple kinetic model does seem to explain some of the features of the unsteady static pressure field.

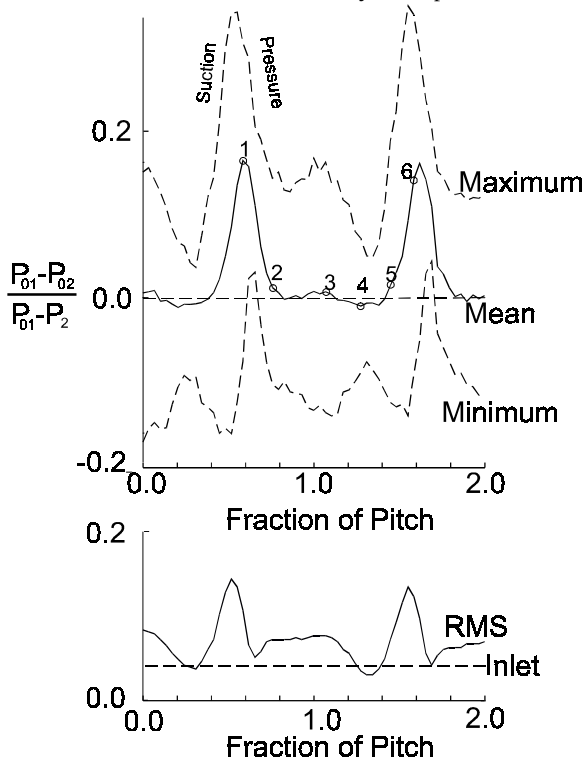

Fig. 7 Time-mean, maximum, minimum and rms of phase-locked average stagnation pressure ½ axial chord downstream of blades - measured

Equations (1) and (2) show that the stagnation pressure and temperature of a particle will change as the particle traverses an unsteady static pressure field (i.e., a non-zero $\partial p / \partial t$ field). Fig. 9 contains, in the upper passage, a contour plot of the quantity $\partial p / \partial t$ at the same instant as fig. 3. In general, the largest values of $|\partial p / \partial t|$ arise near to the leading edge as the wake arrives in that vicinity. However, fig. 3 and fig. 9 do not correspond to that moment. For these figures, a time was chosen when the distortion of the wake-segment within the blade passage is well established. At this instant, fig. 9 shows that the region of most negative $\partial p / \partial t$ lies near to the suction surface, just upstream of region D, the region of highest unsteady static pressure. The region of most positive $\partial p / \partial t$ can be found between the local pressure maximum (region D) and minimum (region B). These regions of positive and negative $\partial p / \partial t$ arise because $\partial p / \partial t$ represents the rate of change of static pressure at a fixed point and the unsteady pressure maximum (region D) and minimum (region B) tend to convect with the main flow.

Contours of the stagnation temperature and stagnation pressure at the same instant as in fig. 3 are presented in the upper and lower passages of fig. 10 respectively. The intervals of the contours of the stagnation quantities represent the same changes of entropy as do the contours in fig. 3. The incoming wakes may be identified using either of the stagnation quantities in fig. 10. Moreover, it requires only a cursory examination of the figure to see that there are much larger

variations within the flow than those associated directly with the entropy defect within the upstream wakes. For example, the difference between the maximum and minimum values of the 'free-stream' stagnation pressure in fig. 10 is approximately five times that of the initial wake-defect. The growth in the magnitude of the stagnation pressure fluctuations could also be seen in the measurements presented in fig. 8. As the wakes do not mix out, changes commensurate with the stagnation pressure changes arise in the stagnation temperature field.

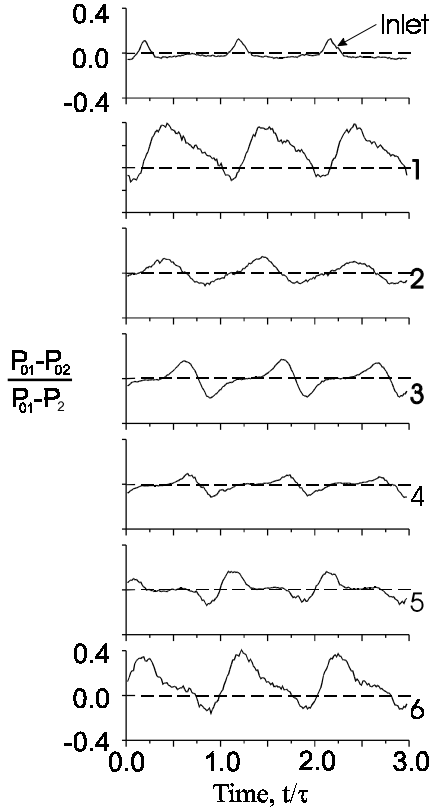

Fig. 8 Phase-locked average stagnation pressure ½ axial chord downstream of blades - measured (for locations, see fig. 7)

The largest perturbations of the stagnation quantities arise near to the suction surface. A comparison of the contour map of $\partial p / \partial t$ in fig. 9 with those of fig. 10, together with equations (1) and (2) explains why this is so. There is a correspondence between the locations of the additional peaks and troughs in the stagnation quantities and the regions of high and low $\partial p / \partial t$. Once created, the peaks and troughs in the stagnation quantities essentially convect with the flow. However, the unsteady static pressure field is partially convective and so is the $\partial p / \partial t$ field. Thus, some particles tend to be convected within a region of mostly positive $\partial p / \partial t$ and so their stagnation pressure and enthalpy tend to increase. Others tend to always be in a region of negative $\partial p / \partial t$ and so the above stagnation quantities will decrease. In this way, the peaks and troughs tend to be reinforced and large amplitude fluctuations of the stagnation quantities begin to appear.

It has been explained that the unsteady static pressure field (strictly, $\partial p / \partial t$) gives rise to variations in time and space of the stagnation pressure and stagnation temperature. It has also been shown the pitchwise variations of the same time-mean stagnation quantities cannot be explained using the negative-jet model of Kerrebrock and Mikolajczak. Though this effect undoubtedly exists, it does not dominate. The cause lies in the nature of the unsteady flow field. On average, more particles on the suction side of the passage experience a more positive $\partial p / \partial t$ for longer than a negative value. This is believed to be associated with the skewed nature of the wake and the unsteady recirculation of the flow that creates a more intense region of low unsteady static pressure on the downstream side of the wake (regions A and B). In a compressor, the distortion effects are much less pronounced and the negative-jet model of Kerrebrock and Mikolajczak may well dominate.

Determination of Loss

We now turn to the question of how to assess thermodynamic loss.

It has been shown that the stagnation pressure and stagnation enthalpy fluctuations that arise due to the unsteady static pressure field are significant in the present context. Fast response pressuretransducer based probes allow us to measure the instantaneous stagnation pressure with relative ease. The measurement of the instantaneous stagnation temperature is much more difficult though possible in specific circumstances. Without the instantaneous stagnation temperature, it will not be possible to distinguish between those changes in stagnation pressure due to unsteadiness and those due to viscous phenomena and so the instantaneous loss cannot be determined.

The time-mean entropy generation is now considered. Applying the 1st Law of thermodynamics to a control volume containing the flow through a whole blade passage at a given instant leads to the result that

$$\left(\dot{Q} - \dot{W}_x\right) = \left(\int_{pitch} h_{02} d\dot{m}_2 - \int_{pitch} h_{01} d\dot{m}_1 \right) + \frac{dE_{CV}}{dt} \qquad (4)$$

where dE_{CV} / dt represents the rate of change of energy (internal plus kinetic) of the control volume. Although there are unsteady forces acting upon the control volume, the point of application of these forces (i.e. the blade surfaces) does not move. Consequently, there is no work transfer. Given that the flow is also adiabatic, the left hand side of eqn. (4) is equal to zero. Integrating the above equation over one wake-passing cycle, leads to the result that

$$\int_{pitch} \overline{h_{02} d\dot{m}_2} = \int_{pitch} \overline{h_{01} d\dot{m}_1} \qquad (5)$$

where the overbars denote the time-mean. Since the time-mean mass flow rate is the same at inlet and at exit, there is no change in the time-mean stagnation enthalpy across the cascade. Equation (5) is true, whether or not the flow is uniform at inlet to or exit from the control volume since no work is transferred.

Here we consider the case of incompressible flow as found in the experiments. For small changes, equations (2) and (5) together lead to the result that the time-mean, pitchwise-averaged entropy change is given by

$$\dot{m}\left(\bar{s}_2 - \bar{s}_1\right) \approx \frac{R}{p_{01}} \left(\int_{pitch} \overline{p_{01} d\dot{m}_1} - \int_{pitch} \overline{p_{02} d\dot{m}_2} \right) \qquad (6)$$

Equation (6) shows that in the case of the experiments described in this paper, it is sufficient to measure the instantaneous change in stagnation

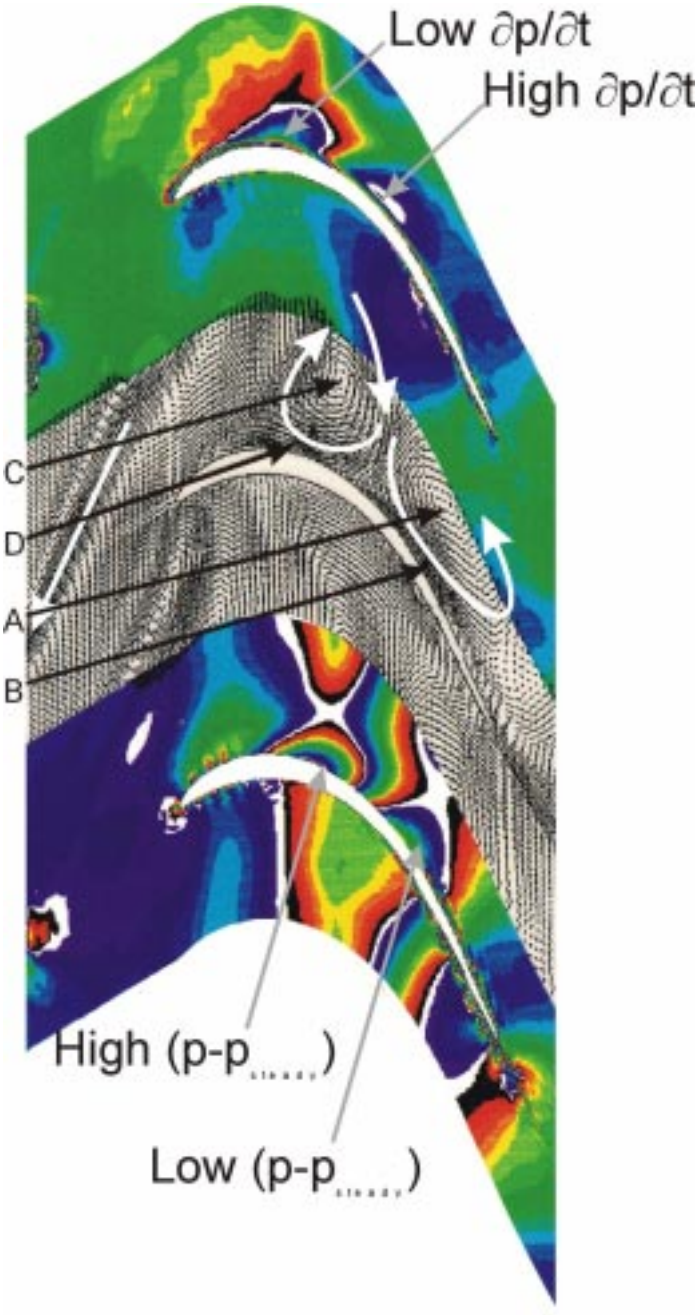

Fig. 9 Contours of $\partial p/\partial t$ (upper) and unsteady static pressure (lower) at same instant as in fig. 3 (contours increase cyclically through black, grey, white)

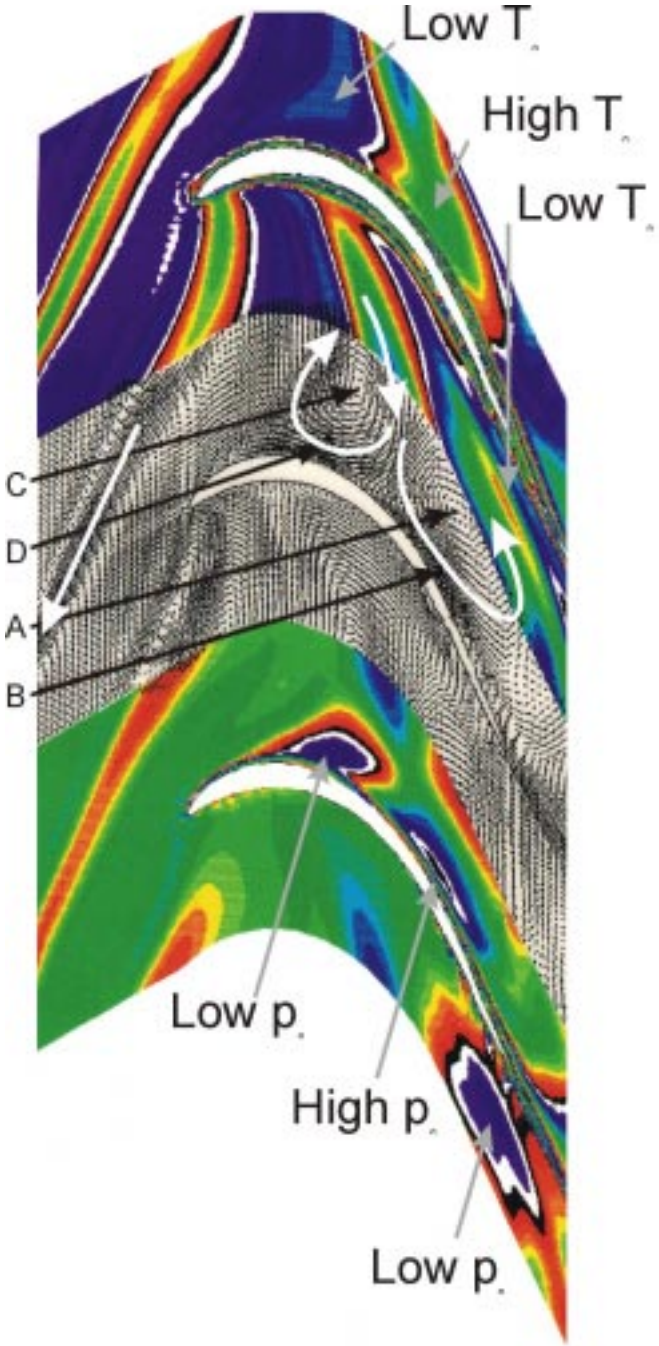

Fig. 10 Contours of absolute stagnation temperature (upper) and absolute stagnation pressure (lower) at same instant as in fig. 3 (contours increase cyclically through black, grey, white)

pressure (and the mass flows) across the stationary cascade in order to evaluate its stagnation pressure loss coefficient. Alternatively, the exit conditions may be determined using conventional pneumatic probes once the unsteady flow has dissipated and become steady.

Unfortunately, the exit flow is rarely steady at the location where exit traverses are made. An assessment of the importance of this aspect can be obtained from a simple calculation that represents the 'worse-case' scenario. A mixing calculation may be performed in which two parallel streams of identical entropy, mass flow and static pressure but different stagnation temperature and stagnation pressure are mixed adiabatically and in the absence of work to form a single stream occupying the same total flow area. The mean stagnation pressure must fall as entropy is created in the mixing process. If the difference in stagnation temperature between the two streams is equal to the maximum amplitude predicted at exit from the cascade ($0.13\ (\bar{T}_{01}\text{-}T_2)$) by the CFD code, then the mixing process generates an entropy increase equivalent to 0.5 percent of the isentropic exit dynamic pressure (i.e., $0.005\ (\bar{P}_{01}\text{-}P_2)$).

In practice, the actual mixing loss associated with the unsteady flow will be less than that calculated above. To investigate this aspect further, an inviscid (Euler) calculation was used to predict the unsteady flow through the cascade. The exit Mach number was again 0.6 in the calculation. The levels of energy separation predicted by this approach were only slightly greater than those predicted by the viscous (Navier-Stokes) method. Mixing out the unsteady flow at the exit of the inviscid flow field generated an increase in entropy equivalent to only 0.25 percent of the exit dynamic pressure. This relatively small rise in entropy indicates that the so-called energy separation that arises in the unsteady flow and which here manifests itself as commensurate changes in stagnation pressure and temperature produces little loss, even at the realistic Mach numbers encountered in the predictions. For comparison, mixing out the incoming wakes at inlet amounts to a loss equal to 0.13 percent of the isentropic exit dynamic pressure (i.e., $0.0013\ (\bar{P}_{01}\text{-}P_2)$). It would seem that for low speed applications at least, and quite probably for higher Mach number cases, it is sufficient to measure the stagnation pressure change across the cascade to determine the entropy creation.

CONCLUSIONS

Measurements of stagnation pressure at exit from a turbine cascade that is subjected to incoming wakes have been presented. The measured exit flow is characterised by the presence of large pitchwise variations in stagnation pressure in the "free-stream", some of which appears as an apparent loss of stagnation pressure towards the pressure side of the passage and some as an apparent gain near the suction side.

The cross-passage transport that is embodied in the negative jet model of Kerrebrock and Mikolajczak is shown to exist but cannot be used to explain the observed non-uniformity in stagnation pressure at the exit from the cascade because it is in the wrong direction.

Predictions and measurements of the unsteady flow field reveal fluctuations in stagnation pressure and stagnation temperature that are greater than the defects that occur in the wake at inlet to the bladerow in question. The large stagnation temperature fluctuations are caused by large variations in $\partial p / \partial t$ which are mostly associated with the suction side flow and are driven by the wake interaction. The flowfield predictions of entropy show little evidence of non-uniformity outside the blade wakes which suggests that many of the stagnation pressure fluctuations are isentropic in origin and therefore related to variations in stagnation temperature. The observed time-mean non-uniformity in stagnation pressure at cascade exit is a direct consequence of these unsteady processes.

Though the fluctuations are relatively large, the time-mean change in stagnation pressure across the cascade is shown to be representative of the entropy generation within the bladerow. The mixing loss associated with the unsteady flow field increases by a factor of two as the wake pass through the bladerow but even at exit, this only amounts to about 0.25 percent of the exit dynamic pressure.

ACKNOWLEDGEMENTS

The authors wish to thank RJ Howell and EM Curtis of the Whittle Laboratory for providing some of the experimental data presented in this paper. They also wish to thank NA Cumpsty for his helpful comments.

REFERENCES

Adachi, T and Murakami, Y, 1979, "Three Dimensional Velocity Distribution Between Stator Blades and Unsteady Force due to Passing Wakes", J S M E, Vol 22 No 170, August, pp 1074-1082

Curtis, EM, Hodson, HP, Banieghbal, MR, Howell, RJ, and Harvey, NW, 1996, "Development of blade profiles for low pressure turbine applications", to be presented at 1996 ASME/IGTI Gas Turbine Congress and Exhibit

Dawes, W N, 1993, "Simulating unsteady turbomachinery flows on unstructured meshes which adapt both in time and space" ASME Paper 93-GT-104, Cincinnati, May

Dawes, W N, 1994, "A numerical study of the interaction of a transonic compressor rotor overtip leakage vortex with the following stator blade row" ASME Paper 94-GT-156, The Hague, June

Dawes, W N, 1994bis, "A simulation of the unsteady interaction of a centrifugal impeller with its vaned diffuser: flow analysis" ASME Paper 94-GT-105, The Hague, June

Dean, RC, 1959, "On the necessity of unsteady flow in fluid machines", Journal of Basic Engineering, March 1959, pp 24-28

Epstein, AH, Giles MB, Shang, T, and Sehra, AK, 1989, "Blade Row Interaction Effects on Compressor Measurements", Proceedings, AGARD Conf PEP 74a on Unsteady Flows in Turbomachines, AGARD CP 468

Giles, M B, 1987, "Calculation of Unsteady Wake/Rotor Interactions, " AIAA Paper 87-0006, presented at AIAA 25th Aerospace Sciences Meeting, Reno, Nevada, 1987

Greitzer, EM, 1984, "An Introduction to the Unsteady Flow in Turbomachines", in "Thermodynamics and Fluid Mechanics of Turbomachinery", AGARD Special Course, Ed by Ucer, A S, and Stow, P

He, L, 1994 "Unsteady Flows and Flutter", Advanced Programme for Industry, Cambridge Univ.

Hodson, H P, 1989, "Modelling Unsteady Transition and Its Effects on Profile Loss", Proceedings, AGARD Conf PEP 74a on Unsteady Flows in Turbomachines, AGARD CP 468

Hodson, HP, 1985, "A Blade-to-Blade Prediction of a Wake-Generated Unsteady Flow", ASME Jnl of Engineering for Gas Turbines and Power, Vol 107, April

Hodson, HP, 1985, "Measurements of Wake-Generated Unsteadiness in the Rotor Passages of Axial Flow Turbines", ASME Jnl of Engineering for Gas Turbines and Power, Vol 107, April

Kerrebrock, JL, and Mikolajczak, AA, 1970, "Intra-Stator Transport of Rotor Wakes and Its Effect on Compressor Performance", ASME Jnl of Engineering for Power, October 1970, pp 359-368

Korakiantitis, T, 1991, "On the Propagation of Viscous Wakes and Potential Flow in Axial-Turbine Cascades" ASME Paper No 91-GT-373

Lopatitskii, A O, et al, 1970, "Energy Losses in the Transient State of an Incident Flow on the Moving Blades of Turbine Stages, " Teploenergetika, Vol 17, No 10, pp 21-23

Meyer, R X, 1958, "The Effect of Wakes on the Transient Pressure and Velocity Distributions in Turbomachines, " ASME Journal of Basic Engineering, October, pp 1544-1552

Rai, M M, 1987, "Navier-Stokes Simulations of Rotor-Stator Interactions using Patched and Overlaid Grids", Jnl Prop Power, Vol 3 No 5, pp 387-396

Schulte, VS, and Hodson, HP, 1996, "Unsteady wake induced boundary layer transition in highly loaded LP turbines", to be presented at 1996 ASME/IGTI Gas Turbine Congress and Exhibit

Smith, L H, 1966, "Wake dissipation in turbomachines", ASME Jnl Basic Engineering, Vol 88D, Sept, pp 688-690

Weyer, H, and Dunker, R, 1983, "Flow measurements in stator rows behind a transonic axial compressor", AGARD CP-351, Viscous Effects in Turbomachines, Copenhagen

Exit Mach number (M_2)	0.6
Exit flow angle (steady flow)	-62.8°
Average loss of incoming wakes	0.035 $\left(\overline{P_{01}} - P_2\right)$
Inlet flow angle (relative)	+62.8°
Inlet flow angle (absolute, free stream)	+30.4°
Inlet flow angle (abs., wake centre-line)	+16.6°
Wake width (= 2*b*)	0.3 x pitch
Max. stagnation pressure defect (rel)	0.05 $\overline{P_{01rel}}$
Max. stagnation pressure defect (abs)	0.019 $\overline{P_{01}}$
Maximum stagnation temp. defect (rel)	0.0 $\overline{T_{01rel}}$
Maximum stagnation temp. defect (abs)	0.0059 $\overline{T_{01}}$
Mesh Size (nodes) per 2-D plane	5000

Table 1 Operating conditions and wake details for turbine calculation

Average loss of incoming wakes (Curtis et al)	0.032 $\left(\overline{P_{01}} - P_2\right)$
Average loss of incoming wakes	0.032 $\left(\overline{P_{01}} - P_2\right)$
Pitch of bars/Cascade Pitch (Curtis et al)	0.57
Pitch of bars/Cascade Pitch	1.15
Inlet flow angle (relative)	+62.8°
Inlet flow angle (absolute - free stream)	+30.4°

Table 2 Wake details for turbine cascade